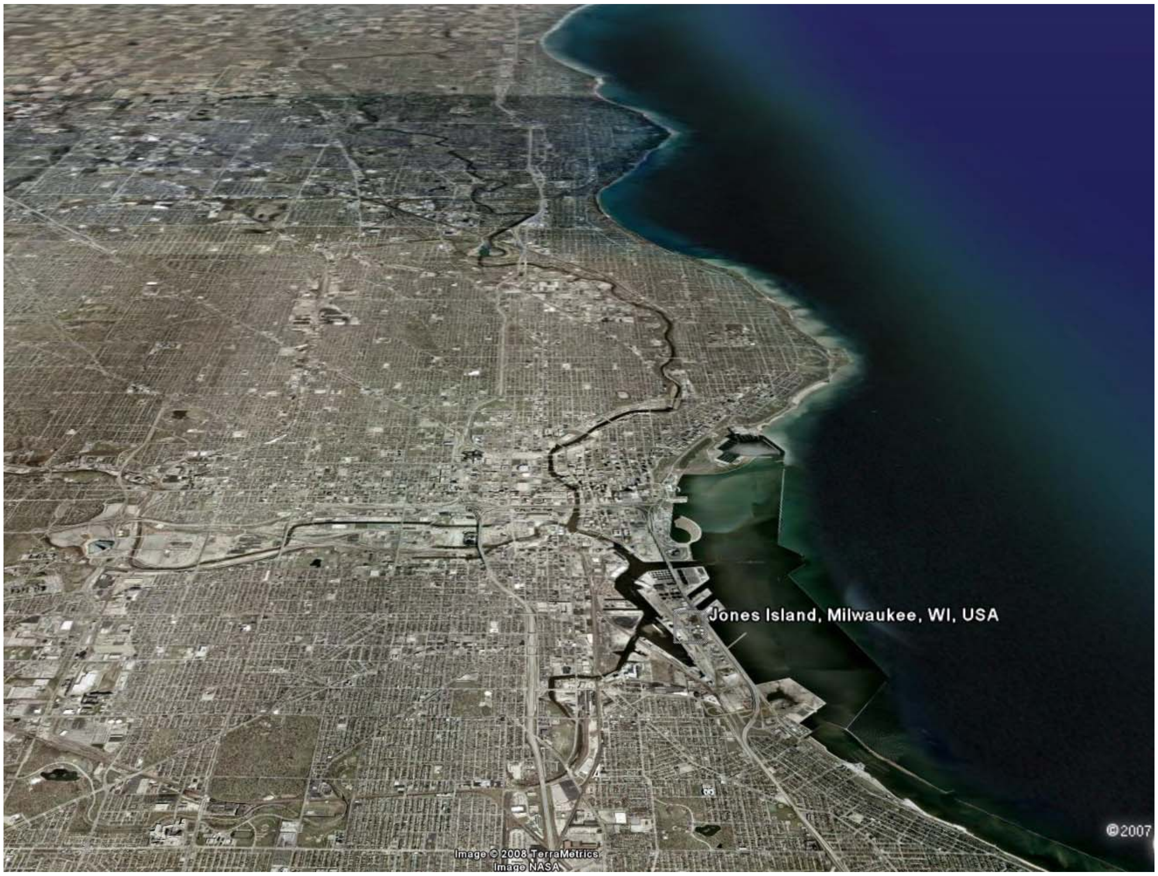

Fellenius, B.H., Riker, R.E., O'Brien, A.O., and Tracy, G.R., 1989. Dynamic and static testing in a soil exhibiting set-up. American Society of Civil Engineers, ASCE, Journal of Geotechnical Engineering, 115(7) 984-1001.

Dynamic and Static Testing in Soil Exhibiting Set-Up

By Bengt H. Fellenius,[1] Richard E. Riker,[2] Arthur J. O'Brien,[3] and Gerald R. Tracy,[4] Members, ASCE

Abstract: Pile foundation studies were conducted on four types of steel piles driven through estuarine deposited soils and into a highly variable glacial deposit to total depths of 33–48 m (110–156 ft). Twenty piles were subjected to dynamic monitoring during initial driving and restriking. For all the monitored piles, static loading tests were carried out to failure and the results compared to ultimate resistances determined in a CAPWAP analysis. With two exceptions, the driving was generally very easy above a depth of 46 m (150 ft). Restriking at different times after driving showed that the penetration resistance increased due to the development of soil set-up occurring within the first week after initial driving and that the final pile capacities vary considerably and randomly across the site. The CAPWAP-determined pile capacities at restriking agreed well with the results of the static loading tests (when the latter could be clearly defined and the hammer had been able to move the pile in the restriking). When the capacity could not be defined in the static test, the CAPWAP determined ultimate resistance was as usable as the conventional methods for determining the load limit of the static test.

Introduction

In 1980, the Milwaukee Metropolitan Sewerage District began an extensive project to upgrade its facilities for intercepting and treating sanitary sewage and stormwater runoff. A significant part of the project involves improvement to the existing Jones Island Wastewater Treatment Plant located near Milwaukee Harbor at the confluence of the Kinnickinnic and Milwaukee Rivers.

The $350 million Jones Island project includes construction of preliminary, primary, and secondary treatment facilities along with modifications to existing facilities. The soil conditions necessitate the installation of 3,000 to 4,000 piles at an estimated cost of $20 million.

Pile foundation studies were conducted during design and construction on four pile types:

1. Normal-wall pipe piles.
2. H-piles.
3. Mandrel-driven pipe piles.
4. Small-diameter heavy-wall pipe piles.

All pipe piles were driven closed toe. The studies integrated conventional static testing with dynamic monitoring and analysis and were performed to select and qualify pile types and hammers, determine pile capacities, and

[1]Prof., Univ. of Ottawa, Dept. of Civ. Engrg., Ottawa, Canada.
[2]CH2M-Hill, Corvallis, OR.
[3]CH2M-Hill, Washington, DC.
[4]CH2M-Hill, Corvallis, OR.

Note. Discussion open until December 1, 1989. To extend the closing date one month, a written request must be filed with the ASCE Manager of Journals. The manuscript for this paper was submitted for review and possible publication on March 8, 1988. This paper is part of the *Journal of Geotechnical Engineering*, Vol. 115, No. 7, July, 1989.

provide reference information to use in construction pile inspection and quality control.

Early in the testing program, it was found that the piles could be driven to bedrock and there obtain a geotechnical capacity in excess of that required. It was also found that the soils exhibited significant increase in pile capacity with time after driving, i.e., soil set-up. Therefore, a secondary purpose of the testing became to find the minimum length of pile required to support the loads (without having to reach the bedrock) for piles with service loads of 90 kN (100 tons). This necessitated that the soil set-up be studied and considered in the design.

The results from nine piles included in the design testing program and from eleven of the production piles are presented in this paper. Fifteen static tests were performed—eight in the initial testing program and seven during driving of production piling. The writers reported the results of preliminary testing programs at the 1983 ASCE conference on Dynamic Measurements of Piles and Piers (Fellenius et al. 1983). These previously published results are summarized herein and compiled with the results of the production pile testing.

General Information

Geotechnical investigations revealed four main strata at the site, as presented in Table 1. The groundwater table lies about 2.5 m (8 ft) below grade and is hydrostatically distributed.

Stratum 2 is a compressible estuarine deposit that varies in thickness and composition between boreholes. All piles were founded in stratum 3, the glacial material, which contains distinct layers or less of comparatively homogeneous clay and silt, sand, and gravel, and heterogeneous mixtures of all these materials. The glacial soil is highly variable in profile and density throughout the project site.

Of the four pile types included in the design phase testing programmes, three were top-driven piles—normal and heavy wall closed-toe (flush end-

TABLE 1. Soil Conditions

Stratum (1)	Type of material (2)	Thickness (3)	Unit weight (4)	Average undrained shear strength (5)	Estimated angle of effective friction (6)
1	Miscellaneous earth fill	15–25 ft	110 pcf	—	30°
2	Soft to medium stiff compressible postglacial silty clay and clayey silt with organics (estuarine)	60–70 ft	105 pcf	800 psf	26–28°
3	Glacial soil deposits	85–95 ft	115 pcf	4,000 psf	35–38°
4	Dolomite bedrock	At depth 165–215 ft	—	—	—

Note: Groundwater table is 8 ft below grade, and pore pressure is hydrostatically distributed; 1 ft = 0.3048 m; and 1 pcf = 0.16 kN/m³.

TABLE 2. Test Piles

Type (1)	Designation (2)	Size (in.) (3)	Area (sq in.) Steel area, A_s (4)	Concrete area, A_c (5)
Thin wall pipe	A	12.75 × 0.375	14.6	113.1
H-pile	B	12 HP63	18.4	0
Thin wall pipe,	C	14.00 × 0.188	8.2	145.8
mandrel-driven		(14.00 × 0.312/lower 20 ft)	13.4	140.5
Heavy wall pipe (small diameter)	D, E, F G, H, I	9.63 × 0.545	15.5	57.2

Note: 1 in. = 25.40 mm; 1 sq in. = 645.2 mm^2; 1 ft = 0.3048 m.

plate) steel pipe piles, and steel H-piles—and one was a mandrel-driven thin-wall pipe pile. The production piles were heavy-wall pipe piles. The design phase test piles have been denoted letters A, B, C, and D, while the production piles have been denoted letters E, F, G, H, and I. Details on these piles are given in Table 2. Fig. 1 shows a plan view of the treatment plant and the locations of the test piles.

The test piles were driven to depths of 33 to 48 m (110 to 156 ft) and the production piles were generally installed to a depth of about 42 to 46 m (140 to 150 ft). The desired service load on the piles in the project ranged from 900 to 1,300 kN (100 to 150 tons).

The A-piles (see Table 2) were driven and restruck with a Vulcan 200C double acting hammer having a nominal (rated) energy of 68 kJ (50 ft-kips). Except as noted, all other piles were driven and restruck with a Vulcan 010 single-acting hammer with a nominal energy of 44 kJ (32.5 ft-kips). Selected restriking of B and C piles was performed with an 71 kN (8 ton) drop-hammer falling 0.9 m (3 ft), i.e., a nominal energy of 65 kJ (48 ft-kips).

Dynamic monitoring using the Pile Driving Analyzer (Goble et al. 1980) was employed during the design phase testing programs as well as during the construction phase. Monitoring was performed during initial driving, as well as during restriking.

Dynamic monitoring of pile driving uses data from transducers attached to the pile near the pile head. The impact from the pile driving hammer produces strain and acceleration in the pile which are picked up by the transducers and transmitted via a cable to the Pile Driving Analyzer placed in a near-by monitoring station. The Analyzer is a computer for acquisition and analysis of the data, translating strain and acceleration to force and velocity and displaying these data on an oscilloscope.

When the force and velocity measured by the analyzer during the impact are plotted as wave traces in a diagram, the incident force and velocity are proportional via the pile impedance (EA/c = area times Young's modulus over wave speed). With the velocity scale proportional to the impedance, initially, force and velocity plot on top of each other. However, when the impact wave meets soil resistance, a portion of the wave is reflected back toward the pile head superimposing the downward traveling wave. Therefore, the reflected force wave in combination with the incident force wave

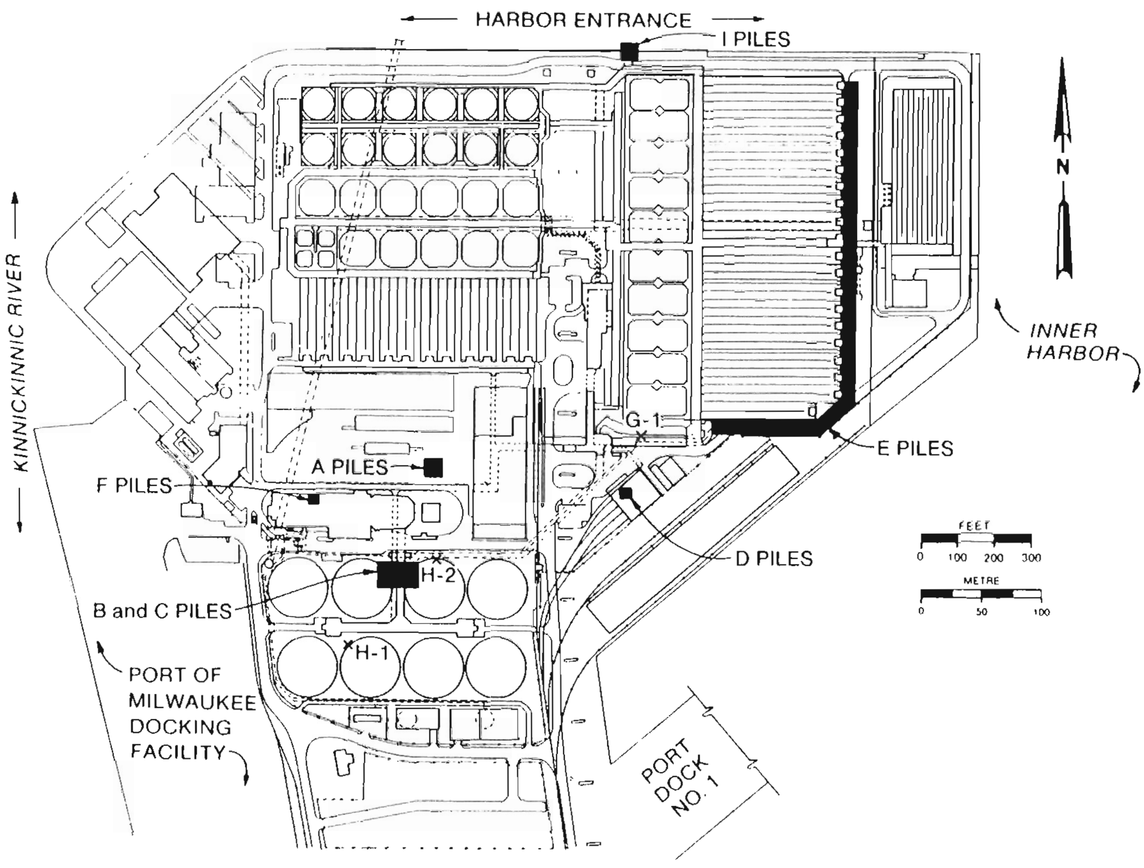

FIG. 1. Plan View of Jonew Island Treatment Plant Showing Test Pile Locations

can exceed the force at impact, i.e., the maximum force be larger than the impact force.

A key to visual interpretation of the wave-trace diagram is that the measured force and velocity traces react differently to the reflection from resistance along the pile: force increases and velocity decreases. The resulting separation of the two traces are, therefore, an indication of the size of the resistance—dynamic and static—and the location and magnitude of shaft resistance is evident from the traces.

The dynamic resistance is a function of pile velocity, called damping. The static resistance depends on the movement, called quake, required to mobilize the ultimate static resistance.

The two measurements—force and velocity—are independent from each other. However, they are caused by the same impact from the hammer and affected by the same soil resistance and they have to follow the same physical laws of wave propagation. The CAPWAP analysis makes use of this situation by means of a signal matching procedure taking as input one measurement, usually the velocity, and moderating it by reflections computed from an assumed distribution of damping, quake, and soil resistance, and transferring it to force by means of wave mechanics computation. Through a trial and error procedure, the input data are adjusted until the computed force trace plots on top of the measured force trace. The CAPWAP analysis has then calibrated the site conditions and provided the static bearing capacity of the pile as well as indicated the dynamic parameters governing the particular hammer/pile/soil combination.

Results

Penetration and Dynamic Monitoring Data

All piles experienced very little penetration resistance in soil strata 1 and 2. In stratum 3, the glacial material, however, the penetration resistance varied considerably between the test locations.

Figs. 2 and 3 show driving diagrams plotted from data obtained during the monitoring of piles A-1 and B-2, respectively, which driving behavior represents the range of driving conditions encountered. The diagram includes the penetration resistance (PRES), the maximum force (FMAX), the impact force (FIMP), and the maximum transferred energy (EMAX), as a function of depth of the pile toe.

Pile A-1 encountered "refusal" driving, i.e., a penetration resistance in excess of 600 blows/m (200 blows/ft) at a relatively shallow depth of 37.5 (123 ft), whereas pile B-2 was terminated at a depth of 47.2 m (155 ft) with a resistance of only 30 blows/m (9 blows/ft). Although a wide range of penetration resistance was obtained on the remaining piles, their driving behavior was generally similar to that of pile B-2.

To avoid testing "refusal" driven piles during the piles A design phase, the driving of piles A-2 and A-4 (compression-test piles) was terminated at a penetration resistance of 26 blows/0.3 m and 45 blows/0.3 m, respectively, at a penetration into the glacial soil about 1.5 m (5 ft) above expected "refusal" level.

Extrapolating from the observations made when driving piles A, it was expected that piles driven at other locations at the site would also meet with practical "refusal" somewhere around the depth of 38 m (125 ft), i.e., in

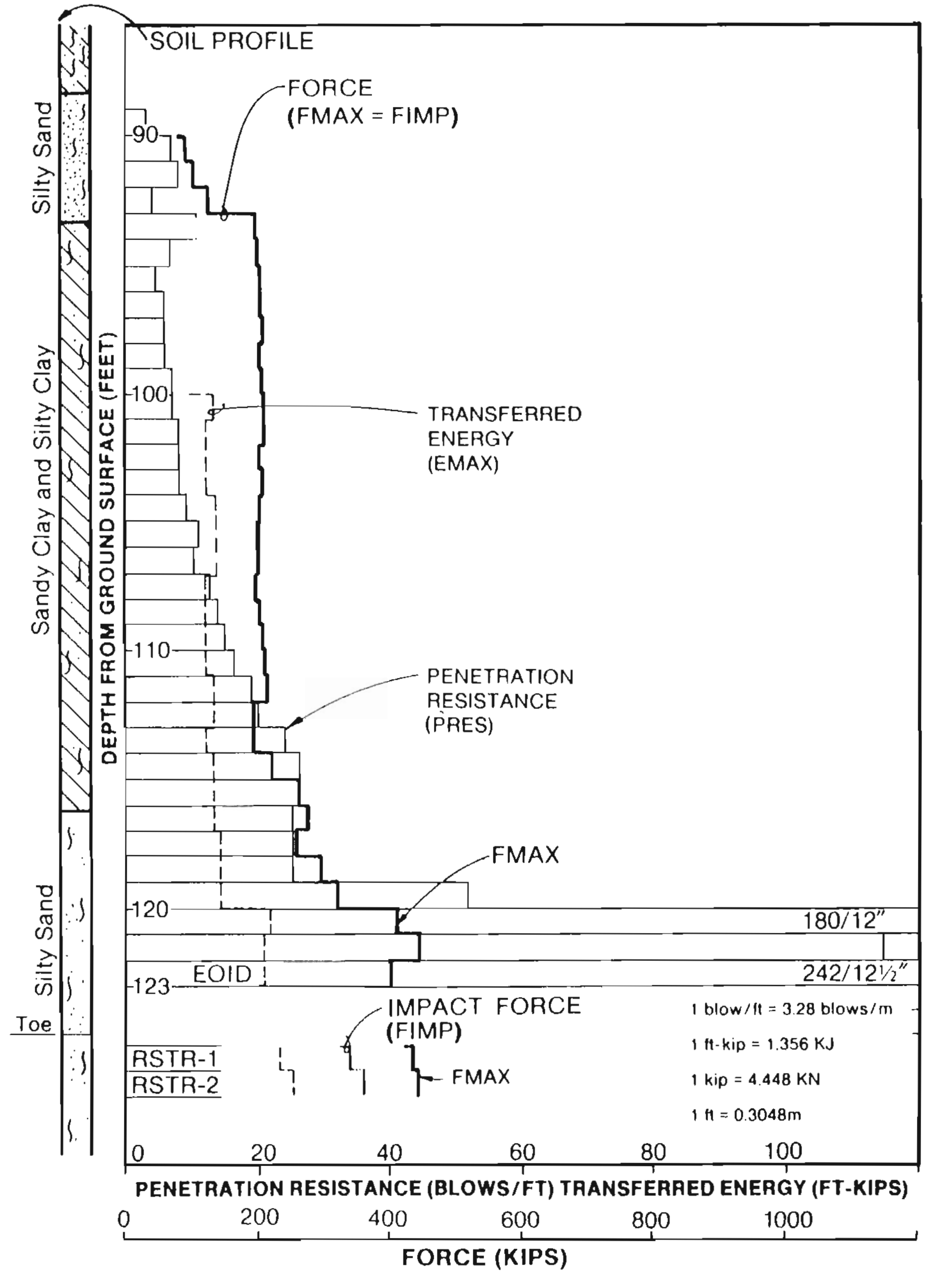

FIG. 2. Driving Diagram for Pile A-1

the dense layer which pile A-1 encountered at the depth of 37.5 m (123 ft). However, and indicative of the highly variable site conditions, in the continued testing at other locations, with the exception of two piles, only moderate penetration resistance was obtained in initial driving above a depth of about 46 m (150 ft). [The exception piles are piles E-3 and E-5. Pile E-3 met "refusal" at a depth of 43.6 m (143 ft) and pile E-5 met "refusal" at 32.3 m (106 ft)].

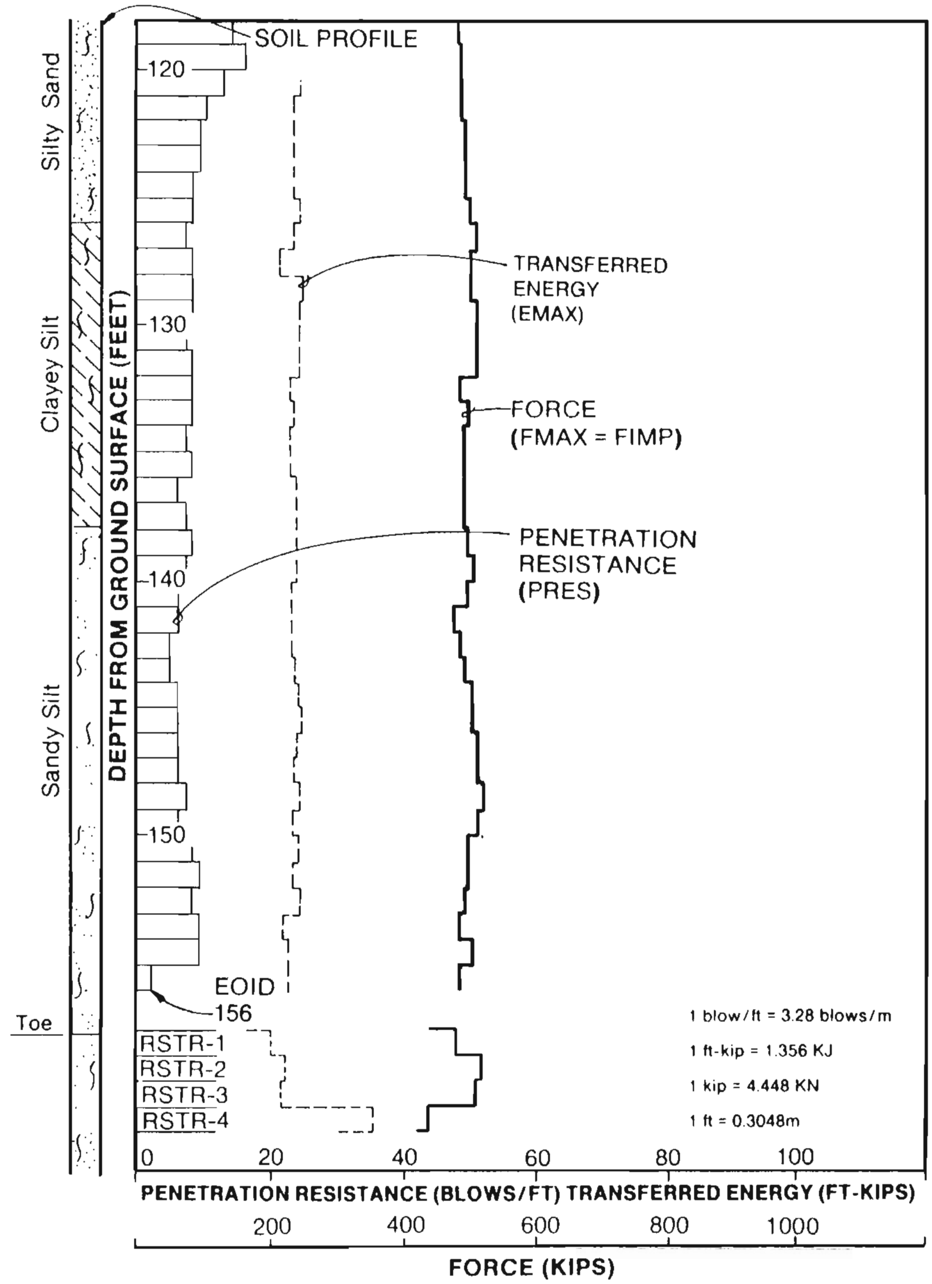

FIG. 3. Driving Diagram for Pile B-2

Table 3 summarizes the driving observations for all test piles.

The driving of test piles B–D and production piles E–I was terminated at "nonrefusal" conditions of penetration resistances (PRES) at end of initial driving (EOID) ranging from 1–5 blows/inch.

To illustrate the observed soil set-up, Figs. 4–6 show wave traces obtained from the end of initial driving (EOID) and restriking (RSTR-1–RSTR-5) of pile B-2. Each set of wave traces shows the measured force and velocity

TABLE 3. Driving Data

Pile (1)	Depth of pile toe (ft) (2)	Driving condition (EOID and RSTR) or static testing (STAT) (3)	Time after EOID (days) (4)	Penetration Resistance (PRES) Blows/in. (5)	Blows/1.0 in. (6)	Hammer type I = 200C II = 010 III = DROP (7)
A-1	123	EOID[a]	—	242/12.00	20	I
		RSTR-1[a]	1	24/0.50	48	I
		RSTR-2[a]	5	20/0.25	80	I
		STAT	12	—	—	
A-2	117	EOID[a]	—	26/12	2	I
		RSTR-1[a]	1	20/1.65	12	I
		RSTR-2[a]	7	190/3.90	49	I
A-3	110	EOID	—	71/12.00	6	I
		STAT	13	—	—	—
A-4	117	EOID[a]	—	45/1200	4	I
		STAT	9	45/12.00	4	—
B-2	155	EOID[a]	—	9/12.00	1	II
		RSTR-1[a]	2	5/2.00	3	II
		RST2-2	6	5/1.00	5	II
		RSTR-3[a]	7	5/0.80	6	II
		STAT	15	—	—	—
		RSTR-4[a]	16	5/1,25	4	III
		RSTR-5-blow #1[a]	132	—	—	II
		RSTR-5-blow #100[a]	132	—	—	II
B-3	142	EOID[a]	—	12/12.00	1	II
		RSTR-1[a]	1	11/5.50	2	II
		STAT (PULL)	7	—	—	—
		RSTR-2[a]	8	6/2.75	2	II
		STAT	10	—	—	—
		RSTR-3[a]	13	3/1.25	2	III
B-4	155	EOID	—	15/12.00	1	II
		RSTR-1[a]	1	5/1.88	3	II
		RSTR-2[a]	9	3/0.63	5	III
C-3	155	EOID	—	21/12.00	2	II
		RSTR-1	1	5/2.40	2	II
		STAT	12	—	—	—
		RSTR-2[a]	13	3/2.00	2	III
		RSTR-3	124	21/4.00	5	II
D-4	156	EOID[a]	—	5/6.00	1	II
		RSTR-1[a]	1	5/1.50	3	II
		STAT	7	—	—	—
E-1	156	EOID	—	18/12.00	2	II
		RSTR-1	5	60/0.20	30	II
		RSTR-2[a]	6	8/0.15	60	II
		STAT	15	—	—	—
E-2	140	EOID	—	55/12.00	5	II
		RSTR-1	8	8/0.25	32	II
		RSTR-2	8	6/0.13	45	II
		RSTR-3[a]	9	6/0.00		—
		STAT	15	—	—	—
E-3	143	EOID[a]	—	225/12.00	19	II
		RSTR-1	1	8/0.25	32	II

TABLE 3. (*Continued*)

(1)	(2)	(3)	(4)	(5)	(6)	(7)
E-4	153	EOID[a]	—	24/12.00	2	II
		RSTR-1[a]	1	5/0.75	7	II
E-5	106	EOID	—	300/12.00	25	II
		RSTR-1[a]	12	7/0.25	28	II
F-1	142	EOID[a]	—	10/12.00	1	II
		RSTR-1[a]	1	10/0.63	16	II
		STAT	51	—	—	—
		RSTR-2[a]	52	50/1.00	50	II
G-1	140	EOID[a]	—	11/12	1	II
		RSTR-1[a]	1	20/1	—	II
		RSTR-2[a]	3	5/	—	II
		STAT	21	—	—	—
H-1	144	EOID	—	6/12	0.5	II
		RSTR-1[a]	5	15/1.3	12	II
		STAT	14	—	—	—
H-2	142	EOID	—	19/12	2	II
		RSTR-1[a]	3	15/		II
		RSTR-2	15	20/		II
I-1	139	EOID	—	14/12	1	II
		RSTR-1[a]	7	40/4	10	II
		STAT	18	—	—	—
I-2	139	EOID	—	13/12	1	II
		RSTR-1[a]	7	28/7	4	II
		RSTR-2	14	25/5	8	II

[a]Signifies that CAPWAP analysis is performed.
Note: 1 blow/ft = 3.28 blows/m; 1 ft = 0.3048 m.

and, for the first four sets, also the transferred energy wave at days 0, 2, 7, 16, and 132. A comparison between the traces indicates clearly that the soil resistance at EOID is small and increases with time after driving, as evidenced by the separation of the force and velocity traces. For a principal discussion on visual interpretation of wave traces, see Rausche et al. (1972), and Authier and Fellenius (1983).

CAPWAP Analyses

Selected wave traces were analyzed using the CAPWAP computer program (Rausche et al. 1972). The results are summarized in Tables 4 and 5. Table 4 gives the evaluated values of stress, energy, and mobilized total, shaft, and toe static resistances.

Table 5 gives the damping factors and quake values used to obtain a CAPWAP match and the calculated maximum toe displacement obtained in the CAPWAP analysis (the calculated maximum toe displacement are not available for piles E and F).

The CAPWAP analysis of the pile capacity assumes that the pile displacement equals or exceeds the soil quake values. However, several of the CAPWAP analyses were performed on data obtained from piles driven against a penetration resistance greater than about 10 blows/in., that is, the maximum pile toe displacement was smaller than the actual soil quake. In such a case,

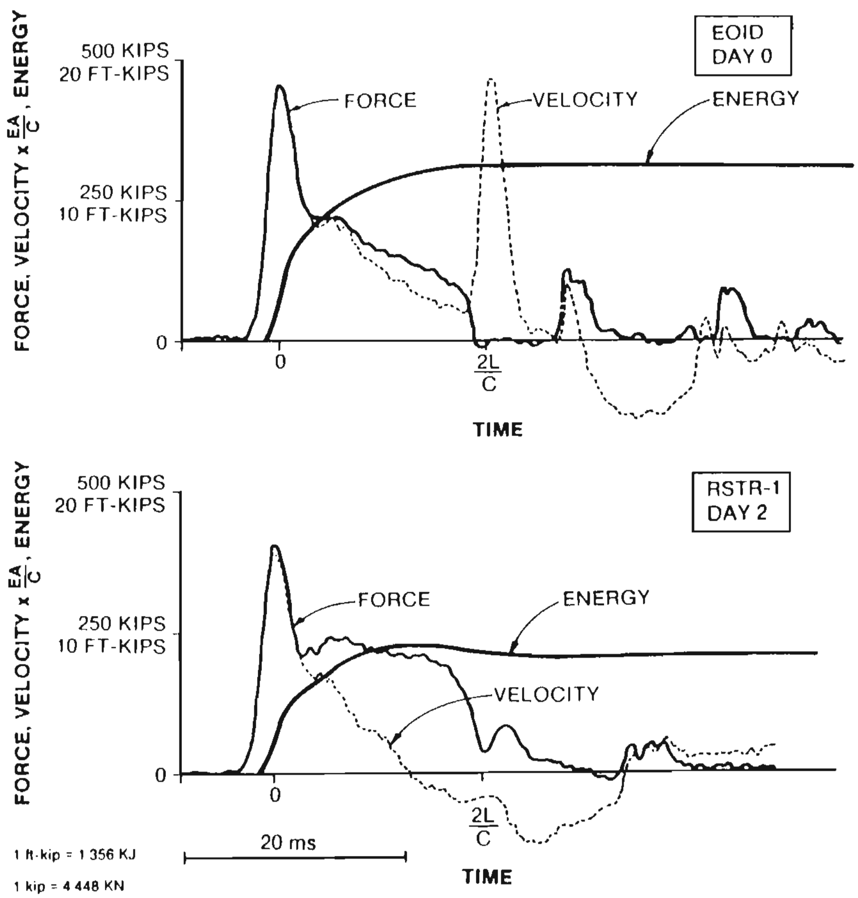

FIG. 4. Pile B-2 Force, Velocity, and Energy Wave Traces (EOID and RSTR-1)

the static soil resistance is not fully mobilized and the CAPWAP determined resistance is smaller than the available ultimate resistance. Such lower bound CAPWAP resistance values are shown in brackets in Table 4. For additional discussion on CAPWAP analysis and quake, see Authier and Fellenius (1980).

Piles *G*, *H*, and *I* were all the same size, installed with the same hammer to essentially the same depth, i.e., 42–44 m (139–144 ft), and all the CAPWAP analyses were performed on driving records taken during restriking (RSTR) within the first seven days after the initial driving. Therefore, it would be expected that the piles should have approximately the same capacity. However, the results of the CAPWAP analyses indicate a spread of ultimate resistance from 1,650 to 2,500 kN (186 to 280 tons), as summarized in Table 4, which further demonstrates the variability of the glacial soils.

Static Loading Tests

Six static axial compression tests were performed during design phase testing using a 4,500 kN (500 tons) loaded platform (dead weight) arrangement. An additional seven compression tests were conducted during production pile driving.

By means of a full length telltale, the displacement of the pile toe was

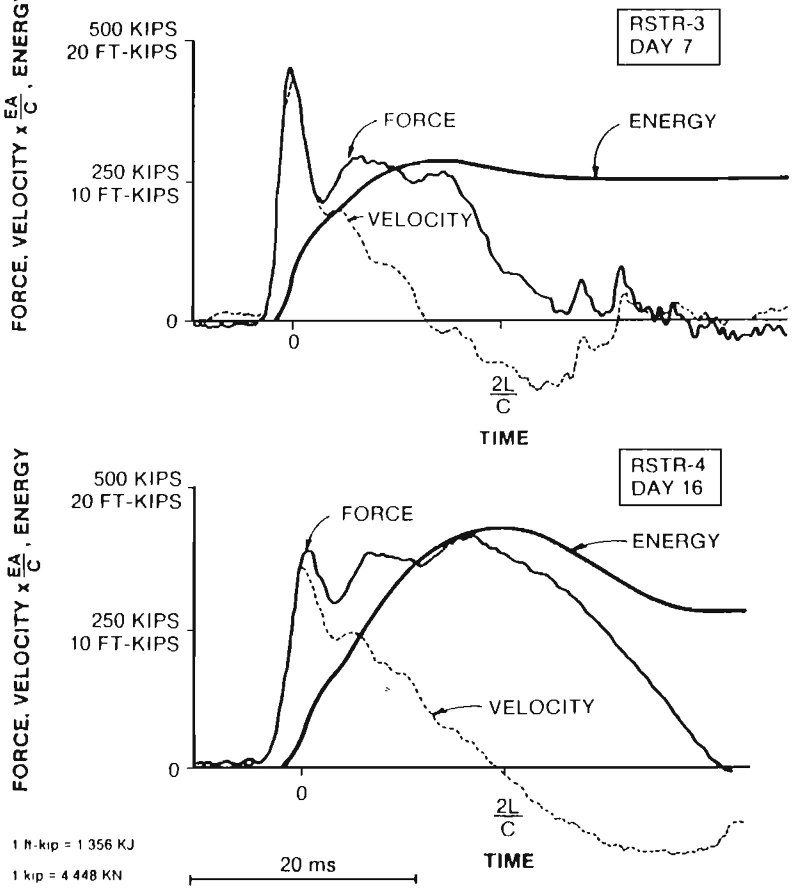

FIG. 5. Pile B-2 Force, Velocity, and Energy Wave Traces (RSTR-3 and RSTR-4)

measured in the axial compression piles. The telltale arrangement followed the recommendations in ASTM D-1143-81.

Two axial tension tests (piles A-3 and B-3) were also performed during design phase testing. These piles were driven in a 9 m (30 ft) deep cased hole to eliminate the direct influence of stratum 1, the fill. As indicated in Table 3, pile B-3 was tested first in compression and then in tension.

The arrangements for the compression and tension tests followed the ASTM D1143-81 and D3689-78 designations, respectively. The quick maintained-load method of testing was applied using small constant increments of load applied every 10 minutes. For compression testing, the range of load increments used was 71 kN (8 tons) for pile F-1 to 133 kN (15 tons) for pile A-1. For tension testing, the load increment was 44 kN (5 tons). All loads were measured by means of a full-bridge strain-gage load cell using the jack manometer only as a back-up gage. The pipe piles were filled with concrete, which was cured for at least 5 days before static testing.

Figs. 7 and 8 show the compression test load-movement behavior of two of the piles, piles A-4 and B-2. The diagrams show the pile-head and pile-toe movements and the compression of the full length of the pile, as measured from the telltales.

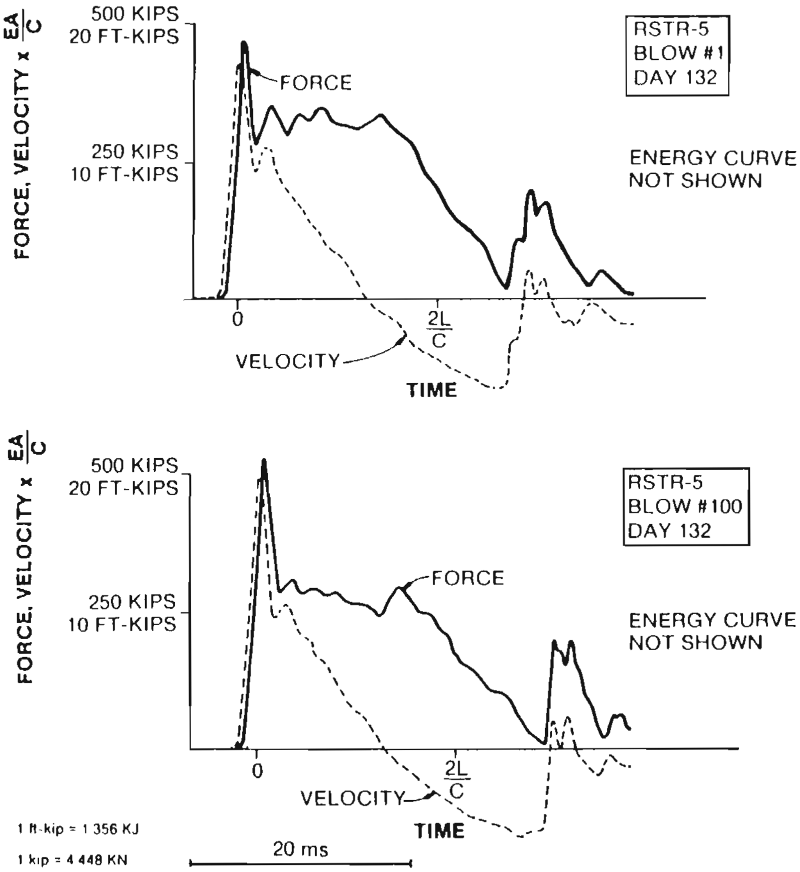

FIG. 6. Pile B-2 Force, Velocity, and Energy Wave Traces (RSTR-5)

The pile-head movement curves were analyzed for load limits using the methods by Davisson, Butler and Hoy, Fuller and Hoy (Nordlund), Brinch-Hansen, and Chin (Kondner), as summarized by Fellenius (1980). The load limits obtained are indicated in the load-movement diagrams.

Most of the compression-tested piles show a load-movement behavior similar to that of pile A-4 (Fig. 7), i.e., the pile-head load-movement is approximately linear up to a head movement of about 25 mm (1.0 in.) and a toe movement of about 10 mm (0.5 in.), whereafter the movement becomes very large for little or no increase in load. In contrast, the test results from piles B-2, B-3, and C-3 do not show this plunging behavior. Instead, the load-movement curve continues to rise in a slightly bending curve even at an appreciably large pile-head movement (120 mm, 5 in., for pile B-2). For these tests, the load limit evaluations (e.g., Brinch-Hansen 80% criterion) indicate that ultimate failure has not been reached.

CAPWAP and Static Test Capacity versus Time

The capacities of the piles as determined by means of CAPWAP analysis and static testing have been compiled in Table 6. The compilation is restricted to the results of the CAPWAP analyses made on blows where the full resistance of the piles was mobilized, i.e, where the calculated maximum

TABLE 4. Summary of Stress, Transferred Energy and Mobilized Static Soil Resistance

Pile (1)	Blow Set (2)	Maximum transferred energy (EMAX) (ft-kips) (3)	Impact Stress (SIMP) (ksi) (4)	Mobilized Static Soil Resistance from CAPWAP (kips) Shaft (5)	Toe (6)	Total (7)
A-1	EOID	28	26	(129)	(261)	(390)
	RSTR-1	28	28	(274)	(191)	(465)
	RSTR-2	31	31	(329)	(189)	(518)
A-2	EOID	16	16	116	96	212
	RSTR-1	25	25	278	144	422
	RSTR-2	19	25	(294)	(113)	(407)
A-4	EOID	25	19	151	120	271
B-2	EOID	25	24	71	39	110
	RSTR-1	18	22	230	40	270
	RSTR-3	21	24	298	42	340
	RSTR-4	35	22	379	71	450
	RSTR-5-blow #1	23	25	(452)	(63)	(515)
	RSTR-5-blow #100	22	28	(406)	(72)	(478)
B-3	EOID	19	23	70	35	105
	RSTR-1	14	18	197	38	235
	RSTR-2	19	22	202	18	220
	RSTR-3	28	20	279	56	335
B-4	EOID	21	20	105	40	145
	RSTR-1	21	22	242	33	275
	RSTR-2	31	23	328	72	400
C-3	RSTR-2	38	—	150	240	390
D-4	EOID	22	27	111	39	150
	RSTR-1	18	25	268	12	340
E-1	RSTR-2	19	24	(416)	(114)	(530)
E-2	RSTR-3	19	23	(376)	(124)	(500)
E-3	EOID	20	25	(115)	(125)	(240)
E-4	EOID	18	21	68	152	220
E-5	RSTR-1	19	26	289	129	418
	RSTR-1	22	26	(252)	(183)	(435)
F-1	EOID	18	25	172	15	187
	RSTR-1	22	26	368	92	460
	RSTR-2	15	26	(510)	(65)	(575)
G-1	EOID	21	24	142	13	155
	RSTR-1	20	25	422	25	447
	RSTR-2	19	23	424	30	454
H-1	EOID	18	24	—	—	—
	RSTR-1	18	20	395	5	400
H-2	EOID	—	—	—	—	—
	RSTR-1	19	24	354	18	372
	RSTR-2	20	22	—	—	—
I-1	EOID	26	26	—	—	—
	RSTR-1	23	25	514	16	530
I-1	EOID	—	—	—	—	—
	RSTR-1	18	20	346	19	365
	RSTR-2	21	25	—	—	—

Note: Parentheses around mobilized static resistance indicate lower bound values, i.e., the toe movement was insufficient to mobilize the full static resistance. 1 kip = 4.448 kN; 1 ft-kip = 1.356 kJ; 1 ksi = 6.895 kPa.

TABLE 5. Summary of Dynamic Soil Parameters

		DAMPING FACTORS						
		Case		Smith		Quake (in.)		Maximum toe displacement (in.) (9)
				Shaft (sec/ft)	Toe (sec/ft)			
Pile (1)	Blow set (2)	Shaft (3)	Toe (4)	(5)	(6)	Shaft (7)	Toe (8)	
A-1	EOID	0.50	0.40	0.101	0.040	0.10	0.15	0.16
	RSTR-1	0.45	0.05	0.43	0.007	0.04	0.04	0.04
	RSTR-2	0.70	0.05	0.055	0.007	0.03	0.03	0.03
A-2	EOID	0.30	0.20	0.067	0.054	0.10	0.20	0.47
	RSTR-1	0.50	0.40	0.047	0.072	0.10	0.25	0.26
	RSTR-2	0.40	0.02	0.035	0.005	0.07	0.06	0.07
A-4	EOID	0.30	0.30	0.052	0.065	0.08	0.75	
B-2	EOID	0.15	0.10	0.071	0.086	0.12	0.12	1.63
	RSTR-1	0.55	0.10	0.080	0.084	0.12	0.12	0.46
	RSTR-3	0.70	0.10	0.079	0.080	0.12	0.12	0.37
	RSTR-4	0.70	0.15	0.065	0.064	0.12	0.12	0.32
	RSTR-5-blow-1	0.95	0.22	0.76	0.126	0.12	0.12	—
	RSTR-5-blow-100	0.78	0.13	0.069	0.065	0.09	0.09	—
B-3	EOID	0.25	0.12	0.120	0.115	0.10	0.10	1.08
	RSTR-1	0.64	0.10	0.109	0.087	0.10	0.10	0.38
	RSTR-2	0.70	0.05	0.116	0.091	0.08	0.10	0.64
	RSTR-3	0.87	0.11	0.104	0.068	0.12–0.22	0.12	0.58
B-4	EOID	0.45	0.10	0.144	0.084	0.12	0.12	0.97
	RSTR-1	0.45	0.07	0.062	0.071	0.12	0.12	0.63
	RSTR-2	0.80	0.10	0.082	0.047	0.12	0.12	0.43
C-3	RSTR-2	0.25	0.10	0.076	0.037	0.12	0.50	0.82
D-4	EOID	0.20	0.15	0.050	0.106	0.15	0.80	0.98
	RSTR-1	0.25	0.70	0.026	0.269	0.15	0.22	0.24
E-1	RSTR-2	0.45	0.35	0.030	0.085	0.06–0.15	0.05	—
E-2	RSTR-3	0.45	0.18	0.033	0.040	0.10	0.10	—
E-3	EOID	0.40	0.30	0.096	0.066	0.15	0.10	—
E-4	EOID	0.27	0.17	0.110	0.031	0.15	0.30	—
	RSTR-1	0.45	0.20	0.043	0.043	0.09	0.09	—
E-5	RSTR-1	0.28	0.22	0.031	0.033	0.10	0.05	—
F-1	EOID	0.02	0.01	0.023	0.133	0.15	0.15	—
	RSTR-1	0.80	0.20	0.064	0.064	0.14	0.14	—
	RSTR-2	0.45	0.45	0.039	0.031	0.15	0.13	—
G-1	EOID	0.39	0.20	0.076	0.045	0.06	0.06	0.90
	RSTR-1	0.95	0.10	0.062	0.111	0.12	0.12	0.10
	RSTR-2	0.90	0.15	0.058	0.138	0.08	0.08	0.09
H-1	EOID	—	—	—	—	—	—	—
	RSTR-1	1.20	0.07	0.085	0.359	0.12	0.08	0.10
H-2	EOID	—	—	—	—	—	—	—
	RSTR-1	0.72	0.06	0.056	0.096	0.06	0.06	0.18
	RSTR-2	—	—	—	—	—	—	—
I-1	EOID	—	—	—	—	—	—	—
	RSTR-1	1.84	0.10	0.099	0.172	0.08	0.05	0.05
	RSTR-2	—	—	—	—	—	—	—

Note: 1 ft = 0.3048 m; 1 in. = 25.40 mm.

toe movement is greater than the quake.

The data are arranged four groups: piles A-2 and A-4, both with length of 36 m (117 ft); piles B-2 and B-4, both with length 47 m (155 ft); piles E-2, F-1, G-1, H-1, H-2, I-1, and I-2, all with a length of about 43 m (140

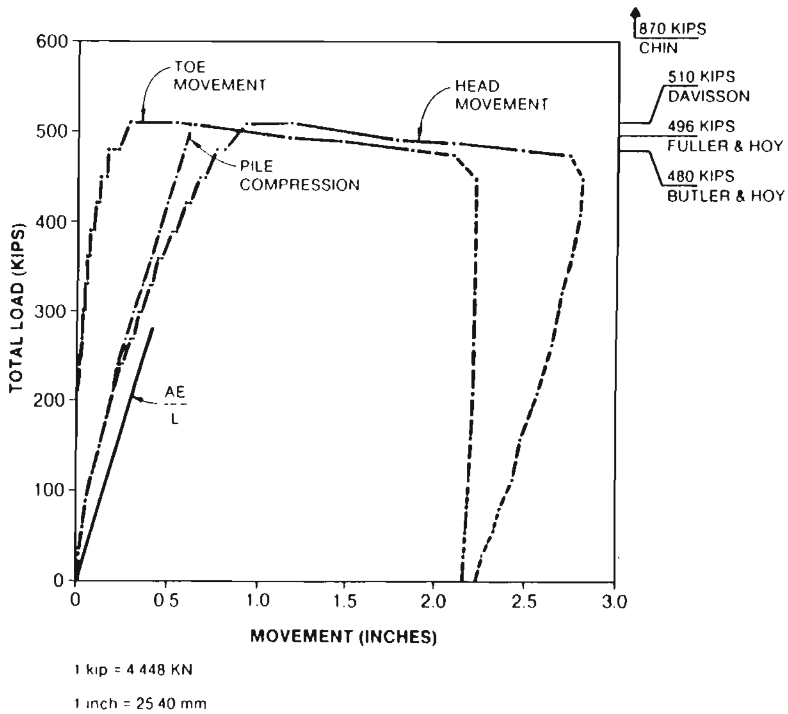

FIG. 7. Pile A-4

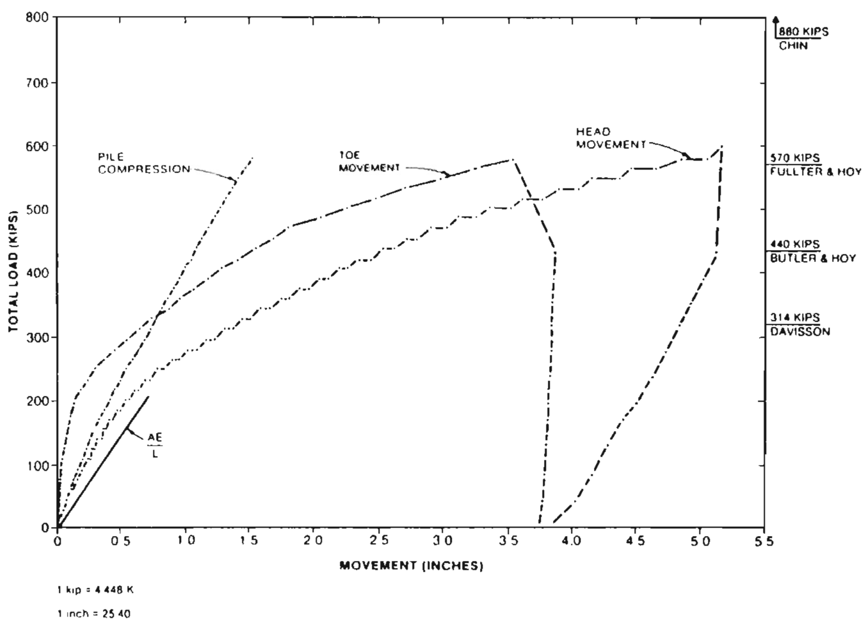

FIG. 8. Pile B-2

TABLE 6. Compilation of Dynamic and Static Testing Data

Pile (1)	Length (ft) (2)	Blow type (3)	Day (4)	Rult (kips) (5)
A-2	117	EOID	0	212
		RSTR-1	1	422
A-4	117	EOID	0	270
		STAT	9	508
B-2	155	EOID	0	110
		RSTR-1	2	270
		RSTR-3	7	340
		STAT	15	314–570
		RSTR-4	16	450
B-4	155	EOID	0	146
		RSTR-1	1	272
		RSTR-2	9	400
E-2	140	STAT	15	660
F-1	142	EOID	0	188
		RSTR-1	1	460
		STAT	51	660
G-1	140	EOID	0	156
		RSTR-1	1	448
		RSTR-2	3	454
		STAT	21	660
H-1	144	RSTR-1	5	400
		STAT	14	380
H-2	142	RSTR-1	3	372
I-1	139	RSTR-1	7	530
		STAT	18	560
I-2	139	RSTR-1	7	366
B-3	142	EOID	0	106
		RSTR-1	1	236
		STAT	10	204–348
		RSTR-3	13	336
E-4	153	EOID	0	220
		RSTR-1	1	418

Note: 1 ft = 0.3048 m; 1 kip = 4.448 kN.

ft); and piles B-3 and E-4, which differ in length from those of the other groups.

The data in Table 6 have been plotted in Fig. 9 showing capacity versus time in days after driving. Three main aspects are evident from this figure. First, the CAPWAP determined capacity increases rapidly over the first day or two, and continues thereafter to increase at a slow but steady rate. Second, there is a considerable scatter between the capacities obtained reflecting the variable soil conditions at the site. See, for instance, the results of static testing of piles E-2 and H-1. These piles are equal in size and length. Yet, the capacity of pile E-2 is almost 75% greater than that of pile H-1, as found in the static loading tests performed on the two piles after about the same number of days after initial driving. Third, and most important, when the effect of time and soil set-up is considered, the CAPWAP determined ca-

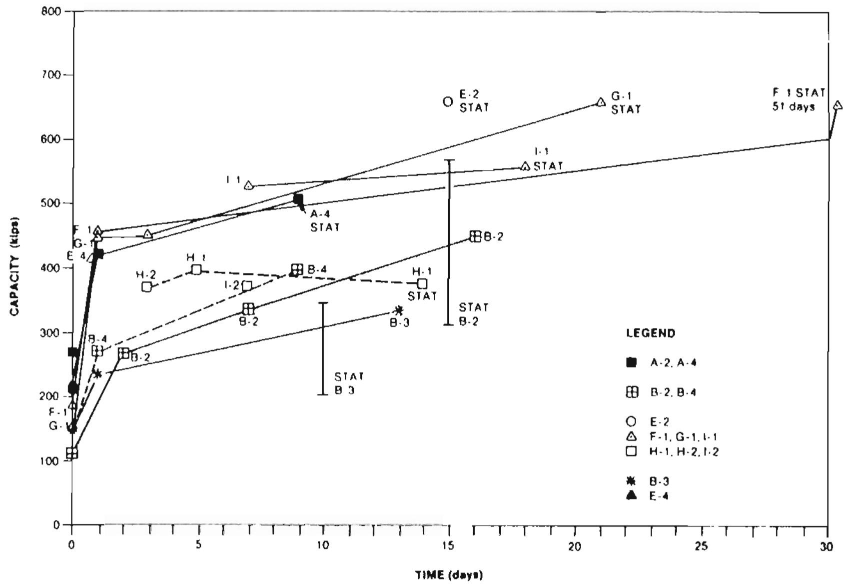

FIG. 9. Capacity versus Time

pacities agree well with the results of the static testing. Where there is a range of load limits found in the static test, the CAPWAP determined capacity is as representative a value as any of the load limits.

The bearing capacity conditions at the site are obviously highly variable. Therefore, had the dynamic monitoring and subsequent CAPWAP analysis not been available to the engineers, it is probable that the variations would have caused severe decision problems at the site during both the design and construction phases. Most certainly, the piles would have been installed much deeper than necessary.

Conclusions

For the piles driven to a depth of about 43 m (140 ft), the initial driving of all but two piles was terminated at a penetration resistance of 1 to 5 blows/in. When restriking the piles, increased penetration resistance was observed indicating the occurrence of soil set-up. The soil set-up was confirmed both visually from the wave traces and in the CAPWAP analyses showing that the increase in resistance was not due to a reduced hammer efficiency or other random influence.

The testing involved seven heavy-wall pipe piles, all about 43 m (140 ft) in length, which were analyzed by means of CAPWAP and five piles tested to failure in static compression loading. Both the capacities determined by means of CAPWAP analysis and by static testing show that the static resistance for the piles varies widely and randomly over the site.

A study of capacity versus days after driving (Fig. 9) shows that the soil set-up occurred rapidly during the first day after initial driving and then continued at a slow but steady rate for at least several weeks.

When comparing the capacities determined in a CAPWAP analysis and a static load test, it is found that the CAPWAP analysis is in good agreement with the results of the static testing, provided the CAPWAP analysis is performed on a blow where the hammer has been able to mobilize the full soil resistance and that the effect of time and soil set-up are considered.

The compilation shown in Fig. 9 indicates that the bearing capacity conditions at the site are highly variable. Had the dynamic monitoring and subsequent CAPWAP analysis not been available to the engineers, it is probable that the variations would have caused severe decision problems at the site during both the design and construction phases.

Acknowledgments

The geotechnical investigations for this project were one element of the overall design of the Jones Island Wastewater Treatment Plant expansion conducted for the Milwaukee Metropolitan Sewerage District (MMSD). Permission of MMSD to present the data is gratefully acknowledged.

The writers wish to thank Edward E. Gillen Company for providing additional restriking beyond their contractual obligations and for valuable assistance in obtaining the data.

Appendix. References

Authier, J., and Fellenius, B. H. (1980). "Quake values determined from dynamic measurements." *Proc. Int. Seminar on the Application of Stress-Wave Theory on Piles,* Stockholm, 1980, H. Bredenberg, Ed., A. A. Balkema, Rotterdam, 197–216.

Authier, J., and Fellenius, B. H. (1983). "Wave equation analysis and dynamic monitoring of pile driving." *Civil Engineering for Practising and Design Engineers,* Vol. 2, Pergamon Press Inc., New York, N.Y., 1–20.

Fellenius, B. H. (1980). "The analysis of results from routine pile loading tests." *Ground Engineering,* Foundation Publishing Ltd., London, 13(5), 395–397.

Fellenius, B. H., et al. (1983). "Dynamic monitoring and conventional pile testing procedures." *Proc., Conf. on Dynamic Measurements of Piles and Piers,* ASCE Spring Convention, Philadelphia, PA.

Goble, G. G., Rausche, F., and Moses, F. (1970). "Dynamic studies on the bearing capacity of piles." Phase III. Report No. 48, Vol. 1 and 2, Division of Solid Mechanics, Structures, and Mechanical Design, Case Western Reserve University, Cleveland, OH.

Goble, G. G., Rausche, F., and Likins, G. E. (1980). "The analysis of pile driving. A state-of-the-art." *Proc., 1st Int. Seminar on the Application of Stress-Wave Theory on Piles,* Stockholm, 1980, H. Bredenberg, Ed., A. A. Balkema, Rotterdam, 131–162.

Rausche, F., Moses, F., and Goble, G. G. (1972). "Soil resistance predictions from pile dynamics." *J. Soil Mech. and Found. Engrg.,* 98(SM9), 917–937.